Ehrenfest-time Dependence of Counting Statistics for Chaotic Ballistic Systems

Daniel Waltner, Jack Kuipers, and Klaus Richter
Institut für Theoretische Physik, Universität Regensburg, D-93040 Regensburg, Germany
(Dated: July 12, 2010)

Transport properties of open chaotic ballistic systems and their statistics can be expressed in terms of the scattering matrix connecting incoming and outgoing wavefunctions. Here we calculate the dependence of correlation functions of arbitrarily many pairs of scattering matrices at different energies on the Ehrenfest time using trajectory based semiclassical methods. This enables us to verify the prediction from effective random matrix theory that one part of the correlation function obtains an exponential damping depending on the Ehrenfest time, while also allowing us to obtain the additional contribution which arises from bands of always correlated trajectories. The resulting Ehrenfest-time dependence, responsible e.g. for secondary gaps in the density of states of Andreev billiards, can also be seen to have strong effects on other transport quantities like the distribution of delay times.

PACS numbers: 03.65.Sq, 05.45.Mt

I. INTRODUCTION

After the conjecture by Bohigas, Gianonni and Schmit in 1984[1], that chaotic systems are well described by Random Matrix Theory (RMT)[2], research started to understand this connection on dynamical grounds by means of semiclassical methods based on analyzing energy averaged products of expressions similar to the Gutzwiller trace formula[3] for the density of states, that are asymptotically exact in the limit $\hbar \to 0$. For open systems we are particularly interested in the scattering matrix $S(E)$, which is an $N \times N$ matrix if the scattering leads carry N states or channels in total. Its elements can, like the Gutzwiller trace formula, be expressed[4] in terms of sums over the classical trajectories containing the stability factors of the orbits A_γ and rapidly oscillating phases depending on the classical actions S_γ of the considered trajectories γ divided by $\hbar$

$$S_{o,i} \approx \frac{1}{\sqrt{T_\mathrm{H}}} \sum_{\gamma(i\to o)} A_\gamma \mathrm{e}^{(\mathrm{i}/\hbar)S_\gamma}, \tag{1}$$

with $T_\mathrm{H} \equiv 2\pi\hbar\Delta$ with the mean level spacing of the quantum system Δ. Here the sum is over the scattering trajectories which connect the two channels i and o. For systems with two (or more) leads the scattering matrix breaks up into reflecting and transmitting subblocks so we might restrict our attention to trajectories starting and ending in certain leads.

In the context of spectral statistics, i.e. for the two point correlation function of the density of states containing a double sum over periodic orbits, this dynamical understanding of the conjecture[1] was - as for other quantities - achieved in several steps. Starting with the pairing of identical (or time reversed orbits in the presence of time reversal symmetry) the so called diagonal contribution was evaluated in Ref. 5 using a sum rule from Ref. 6. Nondiagonal contributions consisting of pairs of long orbits differing essentially only in the place where one of the orbits possesses a self crossing and the other avoids this crossing were analyzed in Ref. 7. This was extended[8] and formalized for orbits differing at several places, so called encounters.

In the context of transport, i.e. for example for the two-point correlator of scattering matrix elements, which if restricted to the transmission subblocks is via the Landauer-Büttiker formalism[9] proportional to the conductance, the diagonal contribution was calculated in Ref. 10. An orbit pair differing only in one crossing was analyzed in Ref. 11 and this was again extended to orbits differing at several places[12]. These results and those for closed systems agreed with results from RMT, but besides this dynamical understanding of the RMT results, these semiclassical calculations proved very successful in determining the effect of a finite Ehrenfest time τ_E on transport quantities, starting with the pioneering work of Ref. 13. The Ehrenfest time[14] separates times where the time evolution of a particle follows essentially the classical dynamics from times where it is dominated by wave interference. Its value is obtained as the time when two points inside a wave packet initially of quantum size $\hbar/p_\mathrm{F}$ with the Fermi momentum p_F evolve to points with a distance L of the linear system size. We thus get due to the exponential separation of neighboring trajectories in the chaotic case

$$\tau_\mathrm{E} = \frac{1}{\lambda} \ln \frac{p_\mathrm{F} L}{\hbar}, \tag{2}$$

with the Lyapunov exponent λ.

Already before these semiclassical calculations of the Ehrenfest-time dependence there existed theories to describe the effect of a finite Ehrenfest time on the correlators of scattering matrix elements: Aleiner and Larkin obtained[15] for the correlator of two transmission matrices, i.e. the conductance, an exponential suppression with increasing Ehrenfest time in agreement with semiclassics. This work was however unsatisfactory in one main aspect: a small amount of impurity scattering was introduced by hand to imitate the effects of diffraction in a ballistic system.

Another phenomenological theory to describe the effect of a finite Ehrenfest time is effective Random Matrix Theory[16]. It splits the phase space and thereby also the underlying scattering matrix of the considered system into a classical and a quantum part, where the first one is determined by all trajectories shorter than $\tau_{\rm E}$ and the second one by all trajectories longer than $\tau_{\rm E}$, as well as introducing an artificial phase dependent on the Ehrenfest time. The predictions of this theory are only partially correct: weak localization is predicted to be independent of the Ehrenfest time, while the previously mentioned theories and also numerical simulations[17,18] predict it to decay with the Ehrenfest time. In contrast to the quantum correction of weak localization, effective RMT gave good predictions for effects at leading order in N like shot noise[19–22] or the gap in the density of states of a chaotic Andreev billiard[23,24].

Staying only at the leading order in inverse channel number we will consider the correlation function of $2n$ scattering matrices at alternating energies defined as

$$C(\epsilon,n,\tau)=\frac{1}{N}\mathrm{Tr}\left[S^\dagger\left(-\frac{\epsilon\hbar}{2\tau_{\rm D}}\right)S\left(+\frac{\epsilon\hbar}{2\tau_{\rm D}}\right)\right]^n, \qquad (3)$$

where for simplicity the energy ϵ is measured with respect to the (Fermi) energy E and in units of the so called Thouless energy $E_{\rm T}=\hbar/2\tau_{\rm D}$ with the dwell time $\tau_{\rm D}$ measuring the typical time a particle stays inside the system. The latter is related to the Heisenberg time $T_{\rm H}$ via the relation $T_{\rm H}=N\tau_{\rm D}$. The Ehrenfest-time dependence is incorporated in $\tau\equiv\tau_{\rm E}/\tau_{\rm D}$. The explicit form is

$$\begin{aligned} C(\epsilon,\tau,n) &= C_1(\epsilon,\tau,n)+C_2(\epsilon,\tau,n), && (4)\\ C_1(\epsilon,\tau,n) &= C(\epsilon,n)\mathrm{e}^{-\tau(1-\mathrm{i}n\epsilon)}, && (5)\\ C_2(\epsilon,\tau,n) &= \frac{1-\mathrm{e}^{-\tau(1-\mathrm{i}n\epsilon)}}{1-\mathrm{i}n\epsilon}, && (6)\end{aligned}$$

with the RMT (i.e. $\tau=0$) part of this correlation function denoted by $C(\epsilon,n)$. The term in (5) derives from effective RMT[16,25]. Although this theory describes certain phenomena quite well, e.g. the dependence of the Andreev gap on the Ehrenfest time[24], a dynamical justification of this result is still lacking. So far Ref. 25 calculated $C(\epsilon,\tau,n)$ for $n=1,2,3$ while Refs. 18,26 showed the separation into two terms in (4) to be a consequence of the preservation under time evolution of a phase-space volume of the system. Moreover they also calculated the explicit form we give in (6) for the second term and that the first term in (5) is proportional to the factor $\mathrm{e}^{-\tau(1-\mathrm{i}n\epsilon)}$.

Because of (1) the correlation function can be written semiclassically in terms of $2n$ scattering trajectories connecting channels along a closed cycle like in Fig. 1a. This leads to trajectory sets with encounters as in Fig. 1b,c which can then be moved into the leads to create the remaining diagrams in Fig. 1. Including the correct prefactors and the energy dependence, the correlation function becomes semiclassically

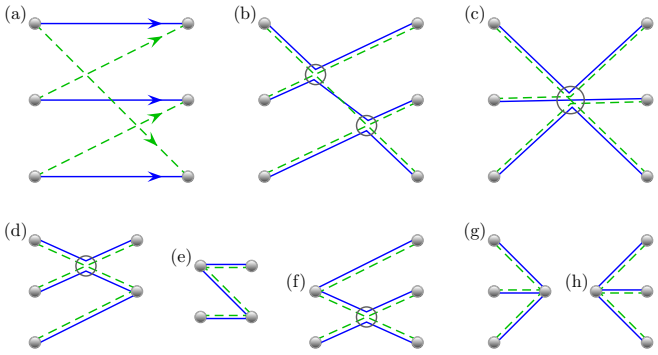

FIG. 1: The trajectory sets with encounters that contribute to the 3rd correlation function $C(\epsilon,3)$

$$C(\epsilon,\tau,n) \approx \frac{1}{NT_{\rm H}{}^n}\prod_{j=1}^{n}\sum_{i_j,o_j}\sum_{\substack{\gamma_j(i_j\to o_j)\\ \gamma'_j(i_{j+1}\to o_j)}} A_{\gamma_j}A^*_{\gamma'_j} \times\mathrm{e}^{(\mathrm{i}/\hbar)(S_{\gamma_j}-S_{\gamma'_j})}\mathrm{e}^{(\mathrm{i}\epsilon/2)(T_{\gamma_j}+T_{\gamma'_j})/\tau_{\rm D}}, \qquad (7)$$

T_γ are the times trajectories γ spend inside the system, and we identify the channels $i_{n+1}=i_1$.

In this paper we want to show how (4,5,6) can be obtained using the trajectory based methods developed in Refs. 7,8,11,12. In Section II we consider the first term in (4): we show that the prefactor $C(\epsilon,n)$ of the exponential is indeed given by the RMT expression obtained in Ref. 27 and that this is multiplied by the exponential given in (5). The underlying diagrams considered here are the same as the ones occurring also in the semiclassical calculation of the RMT contribution. In Section III we consider the second term in (4) and show how this contribution arises from trajectories that are always correlated. Furthermore we show in Section IV that there exist no mixed terms between the first and the second term in (4), that could result - expressed in terms of the considered diagrams - from correlations between trajectories always correlated with each other on the one side and trajectories only correlated with each other during encounters on the other side.

II. INFLUENCE OF THE EHRENFEST TIME ON TRAJECTORIES WITH ENCOUNTERS

The main idea in this Section is to split our diagrams in a different way compared to the semiclassical analysis without Ehrenfest time (referred to as the RMT-treatment) and the analysis of the Ehrenfest-time dependence of the cases $n=1,2,3$ in Ref. 25: in the semiclassical calculation one considers an arbitrary number of orbits encountering each other. It turns out in the RMT-treatment to be sufficient to consider only encounters where all orbits are linearizable up to the *same* point,

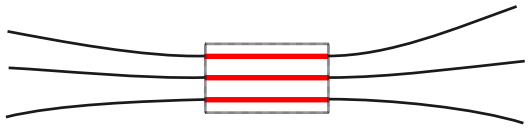

FIG. 2: A 3-encounter as it can be approximated in the RMT-treatment (c.f. Fig. 1c). The encounter stretches are marked by a box (shown red).

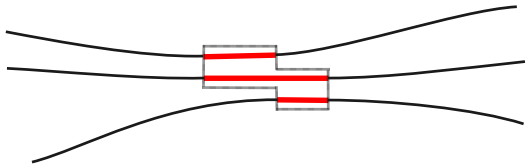

FIG. 3: A 3-encounter as previously treated with Ehrenfest time[25]. The encounter stretches are marked by a box (shown red).

see for an example Fig. 2. When taking into account the Ehrenfest-time dependence this is no longer sufficient as was first shown in Ref. 25, see Fig. 3 for an example of an additional diagram analyzed in this case. The main complication arising in Ref. 25 is then to treat these encounters. In order to simplify the calculation we imagine these encounters being built up out of several encounters which each consist of two encounter stretches, we have distinguished these 2-encounters by different boxes in Fig. 4. In this way it is much easier to consider encounter diagrams of arbitrary complexity with finite Ehrenfest time, which did not appear in the formalism used in Ref. 25.

We first illustrate our procedure by considering three correlated orbits with two 2-encounters as in Fig. 4 and show how the result given in Ref. 25 can be obtained in this case and then treat the general case of n orbits with $(n-1)$ independent or overlapping 2-encounters.

A. Explanation of our procedure for $n = 3$

In the treatment of the RMT-type contribution (5) we first consider the case where all the encounters occur inside the system. For $n = 3$ we have the two semiclassical diagrams in Fig. 1b,c which include a trajectory set (of three original trajectories and three partners) with two 2-encounters in Fig. 1b and a single 3-encounter in Fig. 1c. By shrinking the link connecting the two encounters in Fig. 1b we can see how we deform them into the diagram in Fig. 1c and we use this idea in our Ehrenfest time treatment.

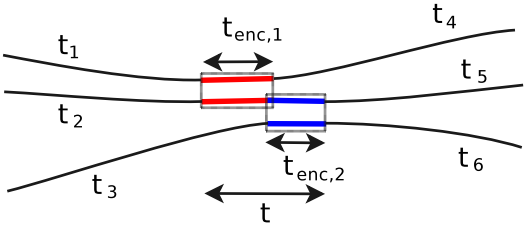

FIG. 4: A diagram with two 2-encounters as we treat it with Ehrenfest time. The encounter stretches of the two 2-encounters are marked by boxes (shown red and blue).

1. *Two 2-encounters*

In our treatment, the overall contribution $C^4(\epsilon,\tau,3)$ of the two 2-encounters (depicted in more detail in Fig. 4) is obtained by allowing the upper trajectory to possess a minimal length of the first 2-encounter and the lowest one a minimal length of the second 2-encounter. The middle trajectory, which passes through both encounters has a minimal length given by the maximum of the two encounter times as we allow the encounters to overlap. However we do not yet allow one encounter to be subsumed into the other so we also set the time t between the start of the first encounter and the end of the second to be longer than the maximum encounter time. To write down the semiclassical contribution of the diagram in Fig. 4 we use the open sum rule[11] and the expected number of times the classical trajectories would approach and form such encounters[12] which gives the simple product

$$\begin{aligned} C^4(\epsilon,\tau,3) \;=\; & \frac{N^2}{\tau_{\rm D}^3}\left(\prod_{i=1}^{6}\int_0^\infty {\rm d}t_i {\rm e}^{-t_i(1-{\rm i}\epsilon)/\tau_{\rm D}}\right) \\ & \times\int_{-c}^{c}{\rm d}^2s{\rm d}^2u\frac{{\rm e}^{{\rm i}\epsilon(t_{{\rm enc},1}+t_{{\rm enc},2})/\tau_{\rm D}}}{\Omega^2 t_{{\rm enc},1}t_{{\rm enc},2}} \\ & \times\int_{\max\{t_{{\rm enc},1},t_{{\rm enc},2}\}}^{\infty}{\rm d}t\,{\rm e}^{({\rm i}/\hbar)\Delta S}{\rm e}^{-t(1-{\rm i}\epsilon)/\tau_{\rm D}}, \end{aligned} \tag{8}$$

where the superscript refers to Fig. 4. We have summed over the possible channels, and t_i with $i = 1,\ldots,6$ label the links from the channels to the encounters. Ω is the volume of available phase space (in the corresponding closed system). In (8) where ${\rm d}^2s = {\rm d}s_1{\rm d}s_2$ and ${\rm d}^2u = {\rm d}u_1{\rm d}u_2$, s_i and u_i with $i = 1,2$ are the stable and unstable coordinate differences between the two parts of the trajectories piercing through a Poincaré surface of section placed in the i-th encounter. Their durations are given by $t_{{\rm enc},i} \equiv \frac{1}{\lambda}\ln\left(c^2/|s_iu_i|\right)$ derived from the condition that the coordinates s_i, u_i are only allowed to grow up to a classical constant c (which is later related to the Ehrenfest time). This separation leads to an action difference $\Delta S = s_1u_1 + s_2u_2 - s_1u_2\exp(-\lambda\Delta t)$, i.e. it also contains products of s,u-coordinates measured in the different Poincaré surfaces of sections where the time Δt

denotes the time the particle needs to travel between the two sections. By expanding the part of the exponential $\mathrm{e}^{(\mathrm{i}/\hbar)\Delta S}$ containing this Δt-dependent part into a Taylor series one verifies easily that contributions from higher order terms than the leading (time independent) one are of higher order in $1/(\lambda\tau_D)$ and can be neglected.

In the first line of (8) we can see that each integral over the links is weighted by its classical probability to remain inside the system for the time t_i which decays exponentially with the average dwell time τ_D. Inside the encounters however we have trajectory stretches which are so close that the conditional survival probability of secondary traversals is 1 and we need only consider the survival probability of one stretch. As the time t (between the two outer ends of the encounter stretches on the middle trajectory shown in Fig. 4) passes through both encounters their survival probability is included in the last line of (8).

Performing the integrals in the first line of (8) we have

$$C^4(\epsilon,\tau,3) = \frac{\tau_\mathrm{D} T_\mathrm{H}^2}{(1-\mathrm{i}\epsilon)^6} F^4(\tau), \tag{9}$$

where we have moved all of the Ehrenfest time dependent parts into the factor $F^4(\tau)$ with the superscript again referring to Fig. 4,

$$\begin{aligned} F^4(\tau) &= \int_{-c}^{c} \mathrm{d}^2 s \mathrm{d}^2 u \frac{\mathrm{e}^{(\mathrm{i}/\hbar)\Delta S} \mathrm{e}^{\mathrm{i}\epsilon(t_{\mathrm{enc},1}+t_{\mathrm{enc},2})/\tau_\mathrm{D}}}{\Omega^2 t_{\mathrm{enc},1} t_{\mathrm{enc},2}} \\ &\quad \times \int_{\max\{t_{\mathrm{enc},1},t_{\mathrm{enc},2}\}}^{\infty} \mathrm{d}t\, \mathrm{e}^{-t(1-\mathrm{i}\epsilon)/\tau_\mathrm{D}}. \end{aligned} \tag{10}$$

Here we can also see the connection with the previous Ehrenfest time treatment of such a diagram. When $t > t_{\mathrm{enc},1} + t_{\mathrm{enc},2}$ the two encounters separate (the integrals can then be further broken down into products) and this is the case where the trajectories can be considered to have two independent 2-encounters as in Ref. 25. Because we choose a different lower limit though, the contribution above also includes some of the diagrams previously treated as 3-encounters in Ref. 25. The reason for our choice becomes clear in the following steps. We first substitute $t' = t - \max\{t_{\mathrm{enc},1}, t_{\mathrm{enc},2}\}$,

$$\begin{aligned} F^4(\tau) &= \int_{-c}^{c} \mathrm{d}^2 s \mathrm{d}^2 u \frac{\mathrm{e}^{(\mathrm{i}/\hbar)\Delta S} \mathrm{e}^{\mathrm{i}\epsilon(t_{\mathrm{enc},1}+t_{\mathrm{enc},2})/\tau_\mathrm{D}}}{\Omega^2 t_{\mathrm{enc},1} t_{\mathrm{enc},2}} \\ &\quad \times \int_0^{\infty} \mathrm{d}t'\, \mathrm{e}^{-(t'+\max\{t_{\mathrm{enc},1},t_{\mathrm{enc},2}\})(1-\mathrm{i}\epsilon)/\tau_\mathrm{D}}, \end{aligned} \tag{11}$$

and then substitute $u_i = c/\sigma_i$, $s_i = c x_i \sigma_i$ and perform the σ_i-integrals using the explicit form of the $t_{\mathrm{enc},i} \equiv \frac{1}{\lambda}\ln\left(c^2/|s_i u_i|\right)$ (for details of this calculation see also Ref. 25). This results in

$$\begin{aligned} F^4(\tau) &= 16 \int_0^1 \mathrm{d}x^2 \frac{\lambda^2 c^4}{\Omega^2} \cos\left(\frac{c^2}{\hbar} x_1\right) \cos\left(\frac{c^2}{\hbar} x_2\right) \\ &\quad \times \int_0^{\infty} \mathrm{d}t'\, \mathrm{e}^{-\left(t'+\max\{-\ln x_1, -\ln x_2\}/\lambda\right)(1-\mathrm{i}\epsilon)/\tau_\mathrm{D}} \\ &\quad \times \mathrm{e}^{-\mathrm{i}\epsilon(\ln x_1 + \ln x_2)/(\lambda\tau_\mathrm{D})}. \end{aligned} \tag{12}$$

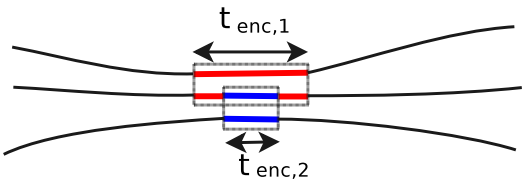

FIG. 5: One 2-encounter is located fully inside the other, corresponding to our treatment of a generalized version of a 3-encounter. The two 2-encounters are marked by boxes (indicated by different colors).

Now we substitute $x_i' = x_i c^2/\hbar$ and obtain

$$\begin{aligned} F^4(\tau) &= 16 \int_0^{\infty} \mathrm{d}x'^2 \frac{\lambda^2\hbar^2}{\Omega^2} \cos(x_1') \cos(x_2') \\ &\quad \times \int_0^{\infty} \mathrm{d}t'\, \mathrm{e}^{-\left(t'+\max\{-\ln x_1', -\ln x_2'\}/\lambda\right)(1-\mathrm{i}\epsilon)/\tau_\mathrm{D}} \\ &\quad \times \mathrm{e}^{-\mathrm{i}\epsilon\left(\ln x_1' + \ln x_2'\right)/(\lambda\tau_\mathrm{D})} \mathrm{e}^{-\tau(1-3\mathrm{i}\epsilon)}. \end{aligned} \tag{13}$$

Here we split the resulting expression into an $\hbar$-independent integral (or more exactly trivially dependent on $\hbar$), that exists due to the energy average that is always contained in our calculations, and an Ehrenfest-time or $\hbar$ dependent part with $\tau_\mathrm{E} \equiv 1/\lambda \ln\left(c^2/\hbar\right)$. This contains the Ehrenfest-time dependence that is expected from (5), so (13) already shows that the diagrams considered here yield the correct Ehrenfest-time dependence.

2. *A 3-encounter*

Now we consider the case that one of the two 2-encounters lies fully inside the other one, which we will refer to as a generalized version of a 3-encounter, as depicted in Fig. 5.

For the Ehrenfest time dependent part we have a similar contribution as in (10) with two differences: First t is best defined as the distance between the midpoints of the two different encounter stretches and so can vary between

$$\begin{aligned} |t| &\leq \frac{1}{2}\left(\max\{t_{\mathrm{enc},1}, t_{\mathrm{enc},2}\} - \min\{t_{\mathrm{enc},1}, t_{\mathrm{enc},2}\}\right), \\ |t| &\leq \frac{1}{2}|t_{\mathrm{enc},1} - t_{\mathrm{enc},2}|. \end{aligned} \tag{14}$$

Second the survival probability of the encounters is determined by the longest encounter stretch and is independent of t. The Ehrenfest time dependent part can then be written as

$$\begin{aligned} F^5(\tau) &= \int_{-c}^{c} \mathrm{d}^2 s \mathrm{d}^2 u \frac{\mathrm{e}^{(\mathrm{i}/\hbar)\Delta S} \mathrm{e}^{\mathrm{i}\epsilon(t_{\mathrm{enc},1}+t_{\mathrm{enc},2})/\tau_\mathrm{D}}}{\Omega^2 t_{\mathrm{enc},1} t_{\mathrm{enc},2}} \\ &\quad \times \int_{-\frac{1}{2}|t_{\mathrm{enc},1}-t_{\mathrm{enc},2}|}^{\frac{1}{2}|t_{\mathrm{enc},1}-t_{\mathrm{enc},2}|} \mathrm{d}t\, \mathrm{e}^{-(\max\{t_{\mathrm{enc},1},t_{\mathrm{enc},2}\})(1-\mathrm{i}\epsilon)/\tau_\mathrm{D}}. \end{aligned} \tag{15}$$

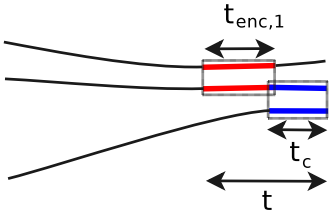

FIG. 6: The second of two 2-encounters now enters the lead so that only t_c of it remains inside the system.

Performing the t integral and following the same steps like for (12,13), we find

$$F^5(\tau) = 16\int_0^\infty \mathrm{d}x'^2 \frac{\lambda^2\hbar^2}{\Omega^2}\frac{|\ln x_1' - \ln x_2'|}{\lambda}\cos(x_1') \times \cos(x_2')\,\mathrm{e}^{-\left(\max\{-\ln x_1', -\ln x_2'\}\right)(1-\mathrm{i}\epsilon)/(\lambda\tau_\mathrm{D})} \times \mathrm{e}^{-\mathrm{i}\epsilon\left(\ln x_1' + \ln x_2'\right)/(\lambda\tau_\mathrm{D})}\mathrm{e}^{-\tau(1-3\mathrm{i}\epsilon)}. \quad (16)$$

Also this part shows an Ehrenfest-time dependence as expected from (5). Note that when performing the t-integral the result in this case is of course proportional to $|t_{\mathrm{enc},1} - t_{\mathrm{enc},2}|$ which contains, after the substitution from x to x', two times the same terms linear in τ_E with different signs that thus cancel each other.

3. *Touching the lead*

Up to now we concentrated on encounters inside the system, but apart from these diagrams we also need to consider diagrams where the encounters touch the opening as in Fig. 1d-h. We will, as above, start with considering encounters built up out of two 2-encounters and focus here on how the calculation of the contribution when encounters move into the lead is changed compared to the treatment of encounters inside the system. As can also be found in more detail in Ref. 25 when encounters touch the lead one includes in the semiclassical expressions for encounters inside the system an additional time integral running between zero and the corresponding encounter time, which characterizes the duration of the part of the encounter stretch that has not yet been moved into the lead.

We consider two encounters with durations $t_{\mathrm{enc},1}$ and $t_{\mathrm{enc},2}$ with the second encounter touching the opening as in Fig. 1d and drawn in more detail in Fig. 6. As the second encounter enters the lead we now define the time t to be from the start of the first encounter until the lead and introduce the time t_c which measures the part of the second encounter that has not yet been moved into the lead. We also separate the Ehrenfest-time relevant contribution $F^6(\tau)$ in this detailed calculation into two cases: in the first case (A); $t_{\mathrm{enc},2} < t_{\mathrm{enc},1}$; we have $F^6_\mathrm{A}(\tau)$ with the additional integral over the time t_c

$$F^6_\mathrm{A}(\tau) = \int_{\substack{-c\\ t_{\mathrm{enc},2}<t_{\mathrm{enc},1}}}^{c} \mathrm{d}^2s\mathrm{d}^2u \frac{\mathrm{e}^{(\mathrm{i}/\hbar)\Delta S}\mathrm{e}^{\mathrm{i}\epsilon t_{\mathrm{enc},1}/\tau_\mathrm{D}}}{\Omega^2 t_{\mathrm{enc},1}t_{\mathrm{enc},2}} \times \int_0^{t_{\mathrm{enc},2}} \mathrm{d}t_c\,\mathrm{e}^{\mathrm{i}\epsilon t_c/\tau_\mathrm{D}} \int_{t_{\mathrm{enc},1}}^\infty \mathrm{d}t\,\mathrm{e}^{-t(1-\mathrm{i}\epsilon)/\tau_\mathrm{D}}, \quad (17)$$

where the limits on the time integrals derive from the fact that the first encounter is not allowed to touch the lead (this would be included as a 3-encounter) and that the second must. Performing the time integrals this is

$$F^6_\mathrm{A}(\tau) = \int_{\substack{-c\\ t_{\mathrm{enc},2}<t_{\mathrm{enc},1}}}^{c} \mathrm{d}^2s\mathrm{d}^2u \frac{\mathrm{e}^{(\mathrm{i}/\hbar)\Delta S}}{\Omega^2 t_{\mathrm{enc},1}t_{\mathrm{enc},2}} \frac{\tau_\mathrm{D}^2}{\mathrm{i}\epsilon(1-\mathrm{i}\epsilon)} \times \left[\mathrm{e}^{\mathrm{i}\epsilon t_{\mathrm{enc},2}/\tau_\mathrm{D}} - 1\right]\mathrm{e}^{-t_{\mathrm{enc},1}(1-2\mathrm{i}\epsilon)/\tau_\mathrm{D}}, \quad (18)$$

with the first and second term in the square brackets resulting from the upper and lower limit of the t_c-integration. In the second case (B); $t_{\mathrm{enc},2} > t_{\mathrm{enc},1}$; we obtain

$$F^6_\mathrm{B}(\tau) = \int_{\substack{-c\\ t_{\mathrm{enc},2}>t_{\mathrm{enc},1}}}^{c} \mathrm{d}^2s\mathrm{d}^2u \frac{\mathrm{e}^{(\mathrm{i}/\hbar)\Delta S}\mathrm{e}^{\mathrm{i}\epsilon t_{\mathrm{enc},1}/\tau_\mathrm{D}}}{\Omega^2 t_{\mathrm{enc},1}t_{\mathrm{enc},2}} \times \left[\int_0^{t_{\mathrm{enc},1}} \mathrm{d}t_c\,\mathrm{e}^{\mathrm{i}\epsilon t_c/\tau_\mathrm{D}} \int_{t_{\mathrm{enc},1}}^\infty \mathrm{d}t\,\mathrm{e}^{-t(1-\mathrm{i}\epsilon)/\tau_\mathrm{D}} + \int_{t_{\mathrm{enc},1}}^{t_{\mathrm{enc},2}} \mathrm{d}t_c\,\mathrm{e}^{\mathrm{i}\epsilon t_c/\tau_\mathrm{D}} \int_{t_c}^\infty \mathrm{d}t\,\mathrm{e}^{-t(1-\mathrm{i}\epsilon)/\tau_\mathrm{D}}\right], \quad (19)$$

where the more complicated limits derive from not allowing the second encounter to move further left than the first. After integrating we have

$$F^6_\mathrm{B}(\tau) = \int_{\substack{-c\\ t_{\mathrm{enc},2}>t_{\mathrm{enc},1}}}^{c} \mathrm{d}^2s\mathrm{d}^2u \frac{\mathrm{e}^{(\mathrm{i}/\hbar)\Delta S}}{\Omega^2 t_{\mathrm{enc},1}t_{\mathrm{enc},2}} \frac{\tau_\mathrm{D}^2}{(1-\mathrm{i}\epsilon)} \times \left[\frac{1}{\mathrm{i}\epsilon}\left[\mathrm{e}^{\mathrm{i}\epsilon t_{\mathrm{enc},1}/\tau_\mathrm{D}} - 1\right]\mathrm{e}^{-t_{\mathrm{enc},1}(1-2\mathrm{i}\epsilon)/\tau_\mathrm{D}} + \frac{1}{(1-2\mathrm{i}\epsilon)}\mathrm{e}^{-t_{\mathrm{enc},1}(1-3\mathrm{i}\epsilon)/\tau_\mathrm{D}} - \frac{1}{(1-2\mathrm{i}\epsilon)}\mathrm{e}^{\mathrm{i}\epsilon t_{\mathrm{enc},1}/\tau_\mathrm{D}}\mathrm{e}^{-t_{\mathrm{enc},2}(1-2\mathrm{i}\epsilon)/\tau_\mathrm{D}}\right]. \quad (20)$$

The last line comes from the upper limit of the second t_c-integral and has the same Ehrenfest-time dependence as before and in line with (5). Likewise the upper t_c time limit for case A in (17) leads to the same dependence and we can conclude that the upper limits of the t_c-integrations yield contributions similar to when the encounters are inside the system and with the same Ehrenfest-time dependence. The remaining (lower) limits of the time integrations in (17,19) give contributions possessing a different Ehrenfest-time dependence which however always yield zero in the semiclassical limit due to the fact that the corresponding terms contain no $t_{\mathrm{enc},2}$

in the exponentials containing $\tau_{\rm D}$. Apart from the action difference, the only term depending on s_2, u_2 is the $1/t_{\rm enc,2}$. The resulting expression is rapidly oscillating as a function of the energy[8] and thus cancelled by the energy average.

We can repeat this procedure for the remaining diagrams in Fig. 1 and see that the contributions are determined by the upper limits of the corresponding t_c integrals. For the diagrams with a generalized 3-encounter (Fig. 1g,h) this follows like for the 3-encounter inside the system but for Fig. 1e where the two 2-encounters enter different channels (and possibly different leads) there is an additional subtlety. The two encounters are still allowed to overlap, so that during the time t the stretch now connecting both channels can always be inside encounters but the individual encounters are not allowed to connect leads at both ends. These additional possibilities are considered later, where if both encounters connect to the leads at both ends we actually have a band of correlated trajectories (treated in Section III) and if only one does we have a mixed term (treated in Section IV). With this organization of the encounters we see that each diagram has the same Ehrenfest-time dependence as when the encounters are inside the system and hence in line with (5).

4. Intermediate summary

The reasoning so far in this Section proves the form of (5) for $n = 3$. First we know that the resulting contribution from the diagrams analyzed contains an overall factor $\mathrm{e}^{-\tau(1-3\mathrm{i}\epsilon)}$, second the remaining integrals are independent of $\hbar$ and thus independent of the Ehrenfest time and third the diagrams we analyze are the same as the ones analyzed in the RMT-case in the first part of 27. As in the limit $\tau_{\rm E} \to 0$ we must recover that previous result, this implies that $C(\epsilon, \tau, 3)$ in (5) is indeed given by the RMT-expression.

5. Full contributions

Before proceeding to the general case, we first however want to illustrate how our calculation can be used to obtain, apart from just the Ehrenfest-time dependence, the complete dependence on $\tau_{\rm D}$ and ϵ.

We therefore start for the two 2-encounters from Fig. 4 from the last expression in (13) and perform first the t'-integral

$$\begin{aligned} F^4(\tau) &= \frac{16\tau_{\rm D}}{(1-\mathrm{i}\epsilon)}\int_0^\infty \mathrm{d}x'^2 \frac{\lambda^2\hbar^2}{\Omega^2}\cos(x_1')\cos(x_2') \\ &\quad\times \mathrm{e}^{-\max\{-\ln x_1', -\ln x_2'\}(1-2\mathrm{i}\epsilon)/(\lambda\tau_{\rm D})} \\ &\quad\times \mathrm{e}^{\min\{-\ln x_1', -\ln x_2'\}\mathrm{i}\epsilon/(\lambda\tau_{\rm D})}\mathrm{e}^{-\tau(1-3\mathrm{i}\epsilon)}, \end{aligned} \quad (21)$$

where it is simpler to rewrite the result in terms of the maximum and minimum value of $\ln x_i'$. For calculating the x_i'-integrals we perform partial integrations (integrating each time the cos functions) and then perform the resulting integrals from zero to infinity

$$\begin{aligned} F^4(\tau) &= -\frac{16\mathrm{i}\epsilon}{\tau_{\rm D}}\frac{(1-2\mathrm{i}\epsilon)}{(1-\mathrm{i}\epsilon)}\int_0^\infty \mathrm{d}x'^2 \frac{\hbar^2}{\Omega^2}\frac{\sin(x_1')}{x_1'}\frac{\sin(x_2')}{x_2'} \\ &\quad\times \mathrm{e}^{-\max\{-\ln x_1', -\ln x_2'\}(1-2\mathrm{i}\epsilon)/(\lambda\tau_{\rm D})} \\ &\quad\times \mathrm{e}^{\min\{-\ln x_1', -\ln x_2'\}\mathrm{i}\epsilon/(\lambda\tau_{\rm D})}\mathrm{e}^{-\tau(1-3\mathrm{i}\epsilon)} \\ &= -\frac{\mathrm{i}\epsilon}{\tau_{\rm D}T_{\rm H}^2}\frac{(1-2\mathrm{i}\epsilon)}{(1-\mathrm{i}\epsilon)}\mathrm{e}^{-\tau(1-3\mathrm{i}\epsilon)}. \end{aligned} \quad (22)$$

In the first line the further terms due the partial integration are either zero or cancel due to the energy average. The final result in the last line of (22) can be also obtained by replacing $\max\{-\ln x_1', -\ln x_2'\}/\lambda = y_1$ and $\min\{-\ln x_1', -\ln x_2'\}/\lambda = y_2$ and performing the integrals with respect to y_i from zero to infinity.

To evaluate the contribution from the generalized 3-encounter in Fig. 5 we again perform two partial integrations in (16) and obtain

$$\begin{aligned} F^5(\tau) &= \frac{16}{\tau_{\rm D}}(1-\mathrm{i}\epsilon)\int_0^\infty \mathrm{d}x'^2 \frac{\hbar^2}{\Omega^2}\frac{\sin(x_1')}{x_1'}\frac{\sin(x_2')}{x_2'} \\ &\quad\times \mathrm{e}^{-\max\{-\ln x_1', -\ln x_2'\}(1-2\mathrm{i}\epsilon)/(\lambda\tau_{\rm D})} \\ &\quad\times \mathrm{e}^{\min\{-\ln x_1', -\ln x_2'\}\mathrm{i}\epsilon/(\lambda\tau_{\rm D})}\mathrm{e}^{-\tau(1-3\mathrm{i}\epsilon)} \\ &= \frac{(1-\mathrm{i}\epsilon)}{\tau_{\rm D}T_{\rm H}^2}\mathrm{e}^{-\tau(1-3\mathrm{i}\epsilon)}, \end{aligned} \quad (23)$$

where we have also left out the terms from the partial integrations which cancel due to the energy average.

With these results we can now show how they connect to the RMT-type results. For this we need to split our diagrams differently and first need the result for an ideal 3-encounter as depicted in Fig. 2 whose contribution was calculated[25] to be

$$F^2(\tau) = -\frac{(1-3\mathrm{i}\epsilon)}{\tau_{\rm D}T_{\rm H}^2}\mathrm{e}^{-\tau(1-3\mathrm{i}\epsilon)}. \quad (24)$$

With the extra factors in (9) it is clear how in the limit $\tau_{\rm E} = 0$ this reduces to the RMT-type result for a 3-encounter as in Ref. 27. All the remaining contributions should be collected together as two 2-encounters, and as the ideal 3-encounter is included in our generalized 3-encounter we first subtract (24) from (23)

$$F^5(\tau) - F^2(\tau) = 2\frac{(1-2\mathrm{i}\epsilon)}{\tau_{\rm D}T_{\rm H}^2}\mathrm{e}^{-\tau(1-3\mathrm{i}\epsilon)}. \quad (25)$$

Before we add the result from our separation of two 2-encounters in (22) we remember that in the treatment we enforce that the first encounter is to the left of the second. The result in (25) does not have this restriction so we divide by 2 to ensure compatibility and then add the result in (22) to obtain

$$F^3(\tau) = \frac{1}{\tau_{\rm D}T_{\rm H}^2}\frac{(1-2\mathrm{i}\epsilon)^2}{(1-\mathrm{i}\epsilon)}\mathrm{e}^{-\tau(1-3\mathrm{i}\epsilon)}. \quad (26)$$

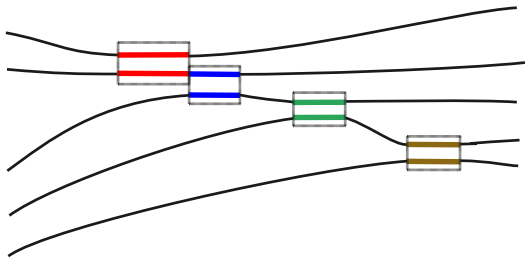

FIG. 7: A ladder of consecutive 2-encounters. The encounter stretches are marked by boxes (shown in different colors).

This then reduces to the RMT-type result for trajectories with two 2-encounters when $\tau_{\rm E}=0$ as in Ref. 27. The agreement of these results with the previous Ehrenfest time treatment[25] can be seen as the result in (26) including both the result from two independent 2-encounters as well as most of the contribution of the diagram referred to as a 3-encounter in Ref. 25. When splitting the contribution in a different way like in Ref. 25 this also leads to terms in both classes that contain different Ehrenfest-time dependencies which only cancel when summed together.

B. All orders

Although up to now we have just reproduced results from Ref. 25, the procedure used here has the advantage that it yields a simple algorithm for determining the Ehrenfest-time dependence of the corresponding contributions to $C_1(\epsilon,\tau,n)$ at arbitrary order. For our example of $n=3$ we showed how it was possible to split the diagrams into two classes that *both* showed the Ehrenfest-time dependence as expected from (5). We want to now show how to generalize our way of splitting considered for 3 trajectories to diagrams containing n trajectories.

1. Ladder diagrams

We start again with the situation where all of the encounters are inside the system and by considering a case analogous to Fig. 4 involving now however n instead of 3 trajectories. We first take a diagram that consists of a ladder of $(n-1)$ 2-encounters so that the central $n-2$ trajectories each contain two encounter stretches while the 2 outside trajectories only contain one encounter stretch each. This situation is depicted in Fig. 7 and the encounters are thus characterized by $(n-1)$ s,u-coordinates.

In this case we obtain for the Ehrenfest-time relevant contribution $F^7(\tau)$ that the t-integral measuring the time difference between the end points of the two encounter stretches on the middle orbit in (10) is replaced by $n-2$ integrals over times t_i with the same meaning as t; they measure the time difference between the end points of the two (consecutive) encounter stretches on the central trajectories containing 2 encounter stretches. These times likewise run from the maximum of the corresponding encounter times to infinity. The survival probability is determined by a single (artificial) stretch that runs through all the encounters so that the exponential term describing the $\tau_{\rm D}$- and ϵ-dependence is now given by

$$\mathrm{e}^{-\sum_{i=1}^{n-2}t_i(1-\mathrm{i}\epsilon)/\tau_D}\mathrm{e}^{\sum_{i=2}^{n-2}t_{\mathrm{enc},i}/\tau_{\rm D}}\mathrm{e}^{\mathrm{i}\epsilon(t_{\mathrm{enc},1}+t_{\mathrm{enc},n-1})/\tau_{\rm D}}, \tag{27}$$

where $t_{\mathrm{enc},i}$ are the durations of the $(n-1)$ individual 2-encounters and the middle exponential compensates for the fact that the middle encounters are traversed by two t_i and that only one traversal should contribute to the survival probability. Setting $t_i'=t_i-\max\{t_{\mathrm{enc},i},t_{\mathrm{enc},i+1}\}$ and repeating now the steps of (12,13) we find the Ehrenfest-time dependent factor in this case to be

$$\begin{aligned}F^7(\tau) &= \left(\frac{4\lambda\hbar}{\Omega}\right)^{n-1}\prod_{j=1}^{n-1}\int_0^\infty \mathrm{d}x_j'\cos\left(x_j'\right)\prod_{i=1}^{n-2}\int_0^\infty \mathrm{d}t_i'\\ &\times\mathrm{e}^{-\sum_{i=1}^{n-2}\left(t_i'+\max\left\{-\ln x_i',-\ln x_{i+1}'\right\}/\lambda\right)(1-\mathrm{i}\epsilon)/\tau_{\rm D}}\\ &\times\mathrm{e}^{-\sum_{i=2}^{n-2}\ln x_i'/(\lambda\tau_{\rm D})}\mathrm{e}^{-\mathrm{i}\epsilon\left(\ln x_1'+\ln x_{n-1}'\right)/(\lambda\tau_{\rm D})}\\ &\times\mathrm{e}^{-\tau(1-in\epsilon)},\end{aligned} \tag{28}$$

again confirming the Ehrenfest-time dependence of (5).

2. Single encounter

Along with the case where none of the encounters in the ladder can move completely inside another we can look at the opposite extreme where all the encounter stretches lie inside of the encounter k with the longest duration $t_{\mathrm{enc},k}=\max_i\{t_{\mathrm{enc},i}\}$ where $t_{\mathrm{enc},i}$ are again the durations of the $(n-1)$ individual 2-encounters. This situation is like a generalization of the diagram in Fig. 5 and we similarly now define the times t_i to be measured between the centers of encounter i and the encounter k of maximum length (with $i\neq k$). Here the same Ehrenfest-time dependence $\mathrm{e}^{-\tau(1-\mathrm{i}n\epsilon)}$ follows by taking into account that each time t_i has a range of variation of size $t_{\mathrm{enc},k}-t_{\mathrm{enc},i}$ and that the $\tau_{\rm D}$- and ϵ-dependent exponential in this case is

$$\mathrm{e}^{-t_{\mathrm{enc},k}(1-\mathrm{i}\epsilon)/\tau_{\rm D}}\mathrm{e}^{\mathrm{i}\epsilon\sum_{i=1}^{n-1}t_{\mathrm{enc},i}/\tau_{\rm D}}. \tag{29}$$

This yields for the Ehrenfest time dependent factor

$$\begin{aligned}F^{7'}(\tau) &= \left(\frac{4\lambda\hbar}{\Omega}\right)^{n-1}\prod_{j=1}^{n-1}\int_0^\infty \mathrm{d}x_j'\cos\left(x_j'\right)\\ &\times\mathrm{e}^{(1-\mathrm{i}\epsilon)\ln x_k'/(\lambda\tau_{\rm D})}\prod_{\substack{i=1\\ i\neq k}}^{n-1}\frac{(\ln x_i'-\ln x_k')}{\lambda}\\ &\times\mathrm{e}^{-\mathrm{i}\epsilon\sum_{i=1}^{n-1}\ln x_i'/(\lambda\tau_{\rm D})}\mathrm{e}^{-\tau(1-in\epsilon)},\end{aligned} \tag{30}$$

confirming again the Ehrenfest-time dependence predicted by (5).

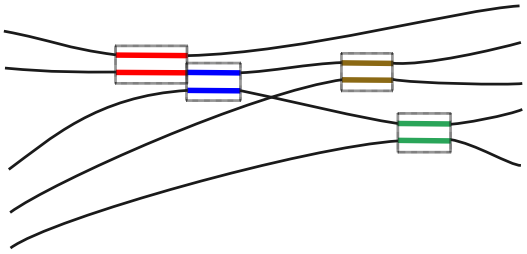

FIG. 8: A general diagram containing encounters marked by boxes (shown in different colors).

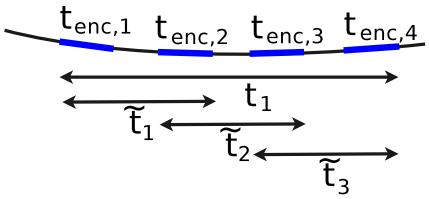

FIG. 9: Definition of the times $\tilde{t}_i$ in the case of more than two encounter stretches on one orbit. The encounter stretches are shown thicker (blue).

3. *Mixture*

Of course it is additionally possible to have a mixed form between these two extreme cases. This means that some 2-encounters only overlap like in the case of a ladder diagram the others form a single encounter. This however just means that some t_i-integrals behave like in the first (ladder) case and some like in the second (single encounter) case. A verification of the predicted Ehrenfest-time dependence is then straightforward.

4. *General encounters*

Up to now we restricted our discussion to diagrams where each trajectory is involved in one or two encounters. This is however not yet the most general case where the only restriction is that each trajectory contains at least one encounter stretch, so that some trajectories can also contain more than two encounter stretches. Note that the situation where two trajectories interact (pass through the same 2-encounter block) more than once cannot occur at leading order in inverse channel number. An example of a diagram that is possible is depicted in Fig. 8. In the most general case we define the times t_i slightly differently: first we separate the $k \geq 2$ trajectories that have one encounter stretch from the remaining $n-k$ that have more than one. Then we number our encounters accordingly, first those along the trajectories with one encounter stretch with duration $t_{\mathrm{enc},i}$, $i = 1 \ldots k$ then the remaining encounters with duration $t_{\mathrm{enc},i}$, $i = k+1 \ldots n-1$. For the $n-k$ trajectories with two or more encounter stretches we now define t_i, $i = 1 \ldots n-k$, to be the time difference between the outer edges of the outermost encounters along those trajectories.

For any trajectories with more than two encounter stretches we will need additional time differences to fully fix the positions of the encounters. Because we defined the times t_i to go through the outmost encounters, importantly the exponential factor with the survival probability and the energy dependence does not depend on these additional time differences and is given by

$$\mathrm{e}^{-\sum_{i=1}^{n-k} t_i(1-\mathrm{i}\epsilon)/\tau_\mathrm{D}} \mathrm{e}^{\sum_{i=k+1}^{n-1} t_{\mathrm{enc},i}/\tau_\mathrm{D}} \mathrm{e}^{\mathrm{i}\epsilon \sum_{i=1}^{k} t_{\mathrm{enc},i}/\tau_\mathrm{D}} \quad (31)$$

where the middle term ensures that the survival probability only includes one copy of each encounter and the energy dependence involves all traversals of all the encounters.

For the remaining times we notice that, starting with the ladder system with 2 trajectories containing one encounter stretch and $n-2$ trajectories containing two stretches, every time we increase the number of trajectories with one encounter stretch we simultaneously increase the number with more than two. Therefore there are $k-2$ additional time differences needed to fix the positions of the central encounters along trajectories with more than two and we define times $\tilde{t}_i$ for $i = 1 \ldots k-2$ from the left hand side of one encounter stretch to the right hand side of the next encounter stretch following on the right on those trajectories, see also Fig. 9. As the encounters are ordered, they are not (yet) allowed to be subsumed by each other or pushed past the outside encounters. The ranges of the times $\tilde{t}_i$ are then fixed by these restrictions. Using $M[i,j] = \max\{t_{\mathrm{enc},i}, t_{\mathrm{enc},j}\}$ in the following to make the notation more compact, we obtain for a trajectory containing m encounter stretches of durations $t_{\mathrm{enc},i}$, $i = 1 \ldots m$, as illustrated in Fig. 9, the integrals

$$\begin{aligned} &\int_{M(1,2)}^{t_i} \mathrm{d}\tilde{t}_1 \ldots \int_{M[m-1,m]}^{t_i - \sum_{o=1}^{m-2}\left(\tilde{t}_o - M[o,o+1]\right)} \mathrm{d}\tilde{t}_{m-1} \\ &= \int_0^{t_i - M[1,2]} \mathrm{d}\tilde{t}'_1 \ldots \int_0^{t_i - \sum_{o=1}^{m-2} \tilde{t}'_o - M[m-1,m]} \mathrm{d}\tilde{t}'_{m-1}. \end{aligned} \quad (32)$$

In the second line we substituted $\tilde{t}'_j = \tilde{t}_j - M[j,j+1]$. The time differences t_i, which are more important for the Ehrenfest-time dependence, must instead just be longer than the maximal length of the encounter stretches lying on the considered trajectory. In general the numbering of the encounters and time differences can be more complicated than in Fig. 9 so we define $l(i)$ to be a list of length $m(i)$ of the encounters enclosed by the time t_i (including the outer encounters) and $L(i)$ a list of the corresponding $m(i)-1$ times $\tilde{t}$ between the ends of those encounters. Now we can make the substitution $t'_i = t_i - \max_{j \in l(i)}\{t_{\mathrm{enc},j}\}$. After this substitution we recognize that (32) has become independent of $\hbar$ or the

Ehrenfest time. Following then the steps in (12,13) we obtain

$$F^8(\tau) = \left(\frac{4\lambda\hbar}{\Omega}\right)^{n-1}\prod_{j=1}^{n-1}\int_0^\infty \mathrm{d}x'_j\cos\left(x'_j\right)\prod_{i=1}^{n-k}\int_0^\infty \mathrm{d}t'_i \times\int_0^{t'_i-\left(\ln x'_{\max,i}+\hat{M}[l_1,l_2]\right)/\lambda}\mathrm{d}\tilde{t}'_{L_1}\ldots \times\int_0^{t'_i-\sum_{o=1}^{m-2}\tilde{t}'_{L_o}-\left(\ln x'_{\max,i}+\hat{M}[l_{m-1},l_m]\right)/\lambda}\mathrm{d}\tilde{t}'_{L_{m-1}} \times\mathrm{e}^{-\sum_{i=1}^{n-k}\left(t'_i-\ln x'_{\max,i}/\lambda\right)(1-\mathrm{i}\epsilon)/\tau_\mathrm{D}} \times\mathrm{e}^{-\sum_{i=k+1}^{n-1}\ln x'_i/(\lambda\tau_\mathrm{D})}\mathrm{e}^{-\mathrm{i}\epsilon\sum_{i=1}^{k}\ln x'_i/(\lambda\tau_\mathrm{D})} \times\mathrm{e}^{-\tau(1-\mathrm{i}n\epsilon)}, \quad (33)$$

with $-\ln x'_{\max,i}=\max_{j\in l(i)}\left\{-\ln x'_j\right\}$ linked to the duration of the longest encounter stretch contained within t_i. We have also defined $\hat{M}[i,j]=\max\left\{-\ln x'_i,-\ln x'_j\right\}$ and dropped the explicit i dependence of l, L and m above. Again we obtain the Ehrenfest-time dependence predicted by (5).

As in the case of the ladder diagram above, we can also have the possibility of some encounter stretches being contained in larger encounter stretches and some separated from those larger encounters. This just implies that some of the t_i integrals have to be treated as was done in the case of the configuration shown in Fig. 5, and the Ehrenfest-time dependence predicted by (5) also follows in this case.

5. *Touching the lead*

When the encounters are allowed to enter the lead we again have to consider times representing how far each encounter has moved into the lead (actually how much of the encounter remains inside the system). As for the case treated in detail for $n=3$ it is only the upper limit (namely the full encounter time) of these time integrals which have the necessary encounter time dependence to contribute in the semiclassical limit. The reasoning for $n=3$ can then be carried over directly to the more general cases as the upper limits of these integrations yield contributions that are (up to constant factors) the same as the ones obtained when the encounters are inside the system. We thus obtain the same Ehrenfest-time dependence from encounters moved into the leads.

C. Summary

The separate diagrams considered in the RMT-type semiclassical treatment[27] can be created from the original collapse of trajectories onto each other and by sliding the individual encounters together or into the leads. The Ehrenfest time treatment however suggests treating all of these possibilities instead as part of continuous families. What we have shown above in this Section is that, if we partition this family in a particular way, for any partition we can find a suitable set of coordinates which allows us to transform the semiclassical contribution so that we can extract the overall Ehrenfest-time dependence. Though the exact details of this transformation depend on the structures of the partition, the algorithmic routines described above all lead to the same Ehrenfest-time dependence. Each partition and hence family then has the factor $\mathrm{e}^{-\tau(1-\mathrm{i}n\epsilon)}$ and no other Ehrenfest time or $\hbar$ dependence. As we know that we must recover the RMT-type result $C(\epsilon,n)$ in (5) when $\tau_\mathrm{E}=0$ (since we treat the same diagrams) with no further Ehrenfest-time dependence, we then obtain the full result in (5) and hence provide a semiclassical justification of the effective RMT Ansatz.

FIG. 10: Band of $n=3$ correlated trajectories. The length of the orbits is marked by a box; the duration of the encounter $t_\mathrm{enc}=1/\lambda\ln\left(c^2/\max_i|s_i|\max_j|u_j|\right)$ is marked by a dotted box.

III. TRAJECTORIES ALWAYS CORRELATED

In this Section we determine the so called classical contribution in (6). To obtain this contribution $C_2(\epsilon,\tau,n)$ semiclassically we consider a band of n trajectories which are correlated (inside the same encounter) for their entire duration between entering and leaving the system as in Fig. 10. This implies that all the trajectories have the same length t and that the maximum of the differences s_i, u_i between their stable and unstable coordinates lies below the constant c (related to the Ehrenfest time). For the case $n=2$ this configuration was first considered in Ref. 22 and then extended to $n=3$ in Ref. 25. For our calculation we follow Ref. 25 and place a Poincaré surface of section at a distance t_1 from the left end of the trajectories while the remaining time on the right of the section is denoted by $t_2=t-t_1$. The semiclassical contribution $C_2(\epsilon,\tau,n)$ can be written as

$$C_2(\epsilon,\tau,n) = \frac{1}{\tau_\mathrm{D}}\int_0^\infty \mathrm{d}t_1\int_0^\infty \mathrm{d}t_2\frac{\mathrm{e}^{-t(1-\mathrm{i}n\epsilon)/\tau_\mathrm{D}}}{(2\pi\hbar)^{n-1}\left(t_1+t_2\right)} \times\int_{|s|\le c\mathrm{e}^{-\lambda t_1}}\mathrm{d}s^{n-1}\int_{|u|\le c\mathrm{e}^{-\lambda t_2}}\mathrm{d}u^{n-1}\mathrm{e}^{(\mathrm{i}/\hbar)\Delta S}, \quad (34)$$

where we only include one traversal of the band in the survival probability and the restrictions on the s and u integrals ensure that the band always remains together under the exponential divergence of the trajectories due to the chaotic dynamics. Performing an integral over

$t_1 - t_2$ and the u_i integrals, this gives

$$C_2(\epsilon,\tau,n) = \frac{4^{n-1}}{\tau_{\rm D}}\int_0^\infty {\rm d}t\,\frac{{\rm e}^{-t(1-{\rm i}n\epsilon)/\tau_{\rm D}}}{(2\pi\hbar)^{n-1}} \times \int_0^{{\rm e}^{-\lambda t}} {\rm d}x^{n-1}\prod_{i=1}^{n-1}\frac{\hbar}{x_i}\sin\left(\frac{c^2 x_i}{\hbar}\right), \quad (35)$$

where $x_i = {\rm e}^{-\lambda t_2}s_i/c$. Using that in the semiclassical limit

$$\int_0^{{\rm e}^{-\lambda t}} {\rm d}x\frac{\hbar}{x}\sin\left(\frac{c^2 x}{\hbar}\right) = \frac{\pi\hbar}{2}\Theta\left(\tau_{\rm E}-t\right), \quad (36)$$

with the Heaviside theta function $\Theta(x)$, we finally obtain

$$C_2(\epsilon,\tau,n) = \frac{1-{\rm e}^{-\tau(1-{\rm i}n\epsilon)}}{1-{\rm i}n\epsilon}, \quad (37)$$

proving the Ehrenfest-time dependence of the $C_2(\epsilon,\tau,n)$ in (6).

IV. MIXED TERMS

Finally we want to consider possible correlations between trajectory structures giving the RMT-type contribution and those giving the classical part, i.e. contributions from correlations between bands of trajectories (that are always correlated with each other) and trajectories that are only correlated with each other during encounters. In particular we want to show that diagrams that have a correlated band which has any encounter with other trajectory structures (with encounters) give no contribution in the semiclassical limit. This, once generalized, then excludes the existence of mixed terms in (4) so that (4) is complete. First we consider the case that $n-1$ of the trajectories form a correlated band with the remaining trajectory meeting the band in an encounter inside the system as depicted in Fig. 11. This contribution $C^{11}(\epsilon,\tau,n)$ to the correlation function $C(\epsilon,\tau,n)$ can be written by treating the correlated band as before and introducing the times t_3 and t_4 to represent the durations of the parts of the trajectory that encounter the band on the left and on the right of the Poincaré surface of section. It reads

$$C^{11}(\epsilon,\tau,n) = \frac{1}{\tau_{\rm D}^3}\int_0^\infty\prod_{i=1}^4{\rm d}t_i\frac{{\rm e}^{-\sum_{i=1}^4 t_i(1-{\rm i}\epsilon)/\tau_{\rm D}}}{(2\pi\hbar)^{n-1}} \times\int_{|s|\le c{\rm e}^{-\lambda t_1}}{\rm d}s^{n-2}\int_{|u|\le c{\rm e}^{-\lambda t_2}}{\rm d}u^{n-2} \times\int_{c{\rm e}^{-\lambda t_1}<|s|\le c}{\rm d}s\int_{c{\rm e}^{-\lambda t_2}<|u|\le c}{\rm d}u \times\frac{{\rm e}^{({\rm i}/\hbar)\Delta S}{\rm e}^{{\rm i}\epsilon(t_{\rm enc}+(n-1)(t_1+t_2))/\tau_{\rm D}}}{t_{\rm enc}\left(t_1+t_2\right)}, \quad (38)$$

where $t_{\rm enc}$ is the time during which the remaining trajectory encounters the band. Performing the integrals as in (35,36) we obtain the Heaviside function $\Theta(\tau_{\rm E}-t)$ from the integral in the second line in (38) over the stable and unstable distances s_i, u_i in the band and the Heaviside function $\Theta(t-\tau_{\rm E})$ from the integral in the third line in (38) over the difference s, u between the coordinates of a band trajectory and the trajectory encountering it. This shows that such a contribution vanishes. If we move more trajectories from the band (composed of at least two trajectories) to the trajectory structure with encounters we still obtain these opposing Heaviside functions and hence no contribution.

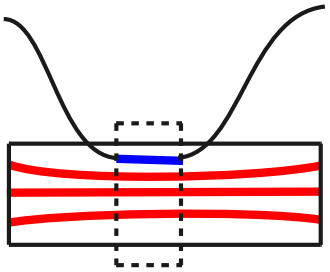

FIG. 11: An example of a band of 3 trajectories that possesses an encounter with another trajectory. The band is marked by a thicker box (red stretches) and the encounter of the other trajectory with the band by a dotted box (blue stretch).

A similar reasoning can be applied if the encounter of a trajectory (or part of a trajectory structure) with a band does not happen inside the system but enters the lead at the beginning or the end. In this case we obtain an additional time integral with respect to the time of the encounter that remains inside the system but, as the s,u-integrals still yield the same Heaviside functions, this contribution also vanishes. Note that if we move both ends of the encounter into the leads then the encountering trajectory can be considered as part of the band and treated as above or in Section III.

The reasoning in this Section applies to an arbitrary number of bands of correlated trajectories connected by trajectories that are only correlated in encounters. Therefore all such mixed terms vanish.

V. IMPLICATIONS FOR TRANSPORT AND SCATTERING

A. Moments of transmission

Up to now we concentrated on energy dependent correlation functions involving the whole scattering matrix. Because we use the same semiclassical diagrams our result can be applied directly to dc-transport properties of chaotic systems like the moments of the transmission or reflection eigenvalues. Assuming the system has two scattering leads and taking just the transmission subblock t of the scattering matrix connecting the N_1 channels in lead 1 to the N_2 channels in lead 2 (without an energy

difference) the moments of the transmission eigenvalues can be written as

$$M(\tau,n)=\frac{1}{N}\mathrm{Tr}\left[tt^{\dagger}\right]^{n}, \tag{39}$$

where $N = N_1 + N_2$ is the total number of channels. Within the Landauer-Büttiker[9] approch to quantum transport the moments carry information about statistical properties of the transmission in the phase coherent regime, the counting statistics[28]. For example the first moment characterizes the average conductance $G \propto M(\tau,1)$ and the second one the power of the shot noise $P \propto M(\tau,1) - M(\tau,2)$. Using the semiclassical results from this article we can simply write

$$M(\tau,n)=M(n)\mathrm{e}^{-\tau}+\frac{N_1N_2}{N^2}\left(1-\mathrm{e}^{-\tau}\right), \tag{40}$$

where we have included the probability N_1/N of starting in lead 1 in the moments. Eq. (40) can be generalized to ac-transport considered in Ref. 29 by including in the latter equation the ϵ-dependent factors given in (5,6). The result in (40) again splits into two parts with the first giving the random matrix probability distribution which comes from the semiclassical moments $M(n)$ calculated in Ref. 30. The second term leads to the classical Bernoulli distribution where the transmission amplitude T is 1 with probability N_2/N and 0 otherwise (i.e. N_1/N). The Ehrenfest time then provides a smooth interpolation between these two distributions giving a weight $\mathrm{e}^{-\tau}$ to the RMT one and the remaining weight $(1-\mathrm{e}^{-\tau})$ to the classical one. A similar formula and result follows for the moments and probability distribution of the reflection eigenvalues whose zero Ehrenfest time contributions can be simply derived from the treatment in Ref. 30.

B. Moments of delay times

Taking the full correlation functions $C(\epsilon,\tau,n)$ it is possible to obtain not only the Ehrenfest-time dependence of the density of states of chaotic Andreev systems, covered in detail in Ref. 27, but also the moments and distribution of the Wigner delay times. We start with the Wigner-Smith matrix[31]

$$Q=\frac{\hbar}{\mathrm{i}}S^{\dagger}(E)\frac{\mathrm{d}S(E)}{\mathrm{d}E}, \tag{41}$$

which can be shown to be Hermitian by using the unitarity of the scattering matrix. Because of this unitarity Q can also be written as

$$Q=\frac{\tau_{\mathrm{D}}}{\mathrm{i}}\frac{\mathrm{d}}{\mathrm{d}\epsilon}\left[S^{\dagger}\left(-\frac{\epsilon\hbar}{2\tau_{\mathrm{D}}}\right)S\left(+\frac{\epsilon\hbar}{2\tau_{\mathrm{D}}}\right)\right]\Big|_{\epsilon=0}, \tag{42}$$

where the scattering matrices energy differences are measured with respect to the energy E. The delay times are simply the eigenvalues of Q so their moments are

$$m(\tau,n)=\frac{1}{N}\mathrm{Tr}\left[Q\right]^{n}. \tag{43}$$

Using the relation

$$\frac{1}{n!}\frac{\mathrm{d}^n}{\mathrm{d}\epsilon^n}\left[f(\epsilon)-f(0)\right]^n\Big|_{\epsilon=0}=\left[f'(0)\right]^n, \tag{44}$$

the moments of the delay times are[32]

$$\begin{aligned} m(\tau,n) &= \frac{\tau_{\mathrm{D}}^n}{\mathrm{i}^n n!N}\frac{\mathrm{d}^n}{\mathrm{d}\epsilon^n}\mathrm{Tr} \\ &\left[S^{\dagger}\left(-\frac{\epsilon\hbar}{2\tau_{\mathrm{D}}}\right)S\left(+\frac{\epsilon\hbar}{2\tau_{\mathrm{D}}}\right)-I\right]^n\Big|_{\epsilon=0}. \end{aligned} \tag{45}$$

Expanding (45), the moments can be expressed as

$$m(\tau,n)=\frac{\tau_{\mathrm{D}}^n}{\mathrm{i}^n n!}\frac{\mathrm{d}^n}{\mathrm{d}\epsilon^n}\sum_{k=1}^{n}(-1)^{n-k}\left(\begin{array}{c}n\\k\end{array}\right)C(\epsilon,\tau,k)\Big|_{\epsilon=0}, \tag{46}$$

in terms of the correlation functions calculated before. As this is additive we can look at the two parts of the Ehrenfest time dependent results in (4) separately.

For the first part of the $C_1(\epsilon,\tau,k)$, though it is possible to put our Ehrenfest dependence into the framework of Ref. 32 where the moments and the probability distribution $\rho(\tau_{\mathrm{W}})$ of the Wigner delay times τ_{W} were calculated (without the Ehrenfest time), we can actually obtain the result in a simple way. Using (44) again we can see that since

$$Q-\tau_{\mathrm{E}}I=\frac{\tau_{\mathrm{D}}}{\mathrm{i}}\frac{\mathrm{d}}{\mathrm{d}\epsilon}\left[S^{\dagger}\left(-\frac{\epsilon\hbar}{2\tau_{\mathrm{D}}}\right)S\left(+\frac{\epsilon\hbar}{2\tau_{\mathrm{D}}}\right)\mathrm{e}^{-\mathrm{i}\epsilon\tau}\right]\Big|_{\epsilon=0}, \tag{47}$$

we have

$$\begin{aligned} \frac{1}{N}\mathrm{Tr}\left[Q-\tau_{\mathrm{E}}I\right]^n &= \frac{\tau_{\mathrm{D}}^n}{\mathrm{i}^n n!}\frac{\mathrm{d}^n}{\mathrm{d}\epsilon^n}\sum_{k=1}^{n} \\ &(-1)^{n-k}\left(\begin{array}{c}n\\k\end{array}\right)C(\epsilon,\tau,k)\mathrm{e}^{-\mathrm{i}k\epsilon\tau}\Big|_{\epsilon=0}. \end{aligned} \tag{48}$$

Plugging in our result for $C_1(\epsilon,\tau,k)$ from (5) the energy dependent exponentials cancel so, apart from the damping factor $\mathrm{e}^{-\tau}$, we just have the moments without any Ehrenfest-time dependence, leading[32] to the RMT result[33]. Of course on the left hand side of (48) we have a simple translation by the Ehrenfest time, meaning that the translated probability distribution is the same as the RMT-one (damped). For the full Ehrenfest-time dependent distribution we simply translate back again and have

$$\begin{aligned} \rho_1(\tau_{\mathrm{W}}) &= \frac{\sqrt{(\tau_+-\tau_{\mathrm{W}})(\tau_{\mathrm{W}}-\tau_-)}}{2\pi(\tau_{\mathrm{W}}-\tau_{\mathrm{E}})^2}\mathrm{e}^{-\tau}, \quad \tau_-<\tau_{\mathrm{W}}<\tau_+ \\ \tau_{\pm} &= (3\pm\sqrt{8})\tau_{\mathrm{D}}+\tau_{\mathrm{E}}. \end{aligned} \tag{49}$$

For the second 'classical' contribution in (4) we first take the simplest part of the contribution

$$C_2^{(1)}(\epsilon,\tau,k)=\frac{1}{1-\mathrm{i}k\epsilon}, \tag{50}$$

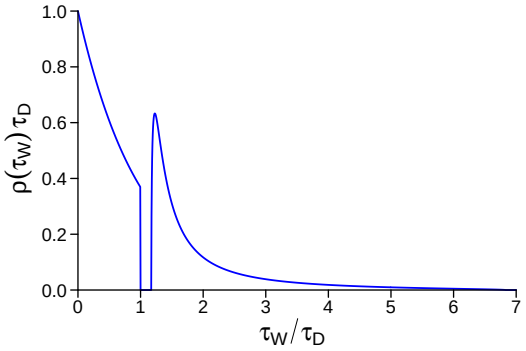

FIG. 12: The probability density of the Wigner delay times for $\tau = 1$.

and substitute into (46) obtaining

$$m_2^{(1)}(\tau, n) = \tau_{\rm D}^n \sum_{k=1}^{n} (-1)^{n-k} \left(\begin{array}{c} n \\ k \end{array} \right) k^n = \tau_{\rm D}^n n!. \qquad (51)$$

These moments clearly come from an exponential distribution, so that in the limit $\tau \to \infty$ we recover, for the probability distribution $\rho_2^{(1)}(\tau_{\rm W})$, the classical exponential decay of trajectories inside the system

$$\rho_2^{(1)}(\tau_{\rm W}) = \frac{1}{\tau_{\rm D}} {\rm e}^{-\tau_{\rm W}/\tau_{\rm D}}. \qquad (52)$$

For the remaining contribution of the second part $\rho_2^{(2)}(\tau_{\rm W})$, we have the damping factor ${\rm e}^{-\tau}$, and the energy dependent phase again just leads to a shift in the exponential distribution so this contribution starts at $\tau_{\rm E}$, thus yielding

$$\rho_2^{(2)}(\tau_{\rm W}) = -\frac{1}{\tau_{\rm D}} {\rm e}^{-\tau_{\rm W}/\tau_{\rm D}}, \quad \tau_{\rm W} > \tau_{\rm E}. \qquad (53)$$

The minus sign however means we truncate the previous exponential at $\tau_{\rm E}$, so the total second contribution to the probability distribution is

$$\rho_2(\tau_{\rm W}) = \frac{1}{\tau_{\rm D}} {\rm e}^{-\tau_{\rm W}/\tau_{\rm D}}, \quad 0 < \tau_{\rm W} < \tau_{\rm E}, \qquad (54)$$

and 0 elsewhere. Since this contribution to the time delay probability distribution is made up of the two distributions $\rho_1^{(1)}(\tau_{\rm W})$ and $\rho_1^{(2)}(\tau_{\rm W})$ and as the shifted and damped one $\rho_1^{(2)}(\tau_{\rm W})$ has the same mean $(\tau_{\rm D} + \tau_{\rm E})$ as the shifted and damped RMT distribution $\rho_1(\tau_{\rm W})$ but a minus sign, it is clear that the average time delay stays at $\tau_{\rm D}$ (i.e. from the untruncated exponential distribution) and is unaffected by the Ehrenfest time.

This shape of the distribution is however significantly affected and as an example we plot the complete probability density of the Wigner delay times for $\tau = 1$ in Fig. 12. There we can see the exponential decay truncated at $\tau_{\rm E} = \tau_{\rm D}$ before a hard gap separates it from the damped RMT distribution which is shifted to the right by $\tau_{\rm E}$.

VI. CONCLUSIONS

In this article we have shown how to treat the effect of the Ehrenfest time on correlation functions of arbitrarily many pairs of scattering matrices. In our semiclassical approach we extended and combined the zero Ehrenfest time approach[27] (which leads to the RMT result) and the $n = 3$ Ehrenfest time approach[25] and showed how the results of the effective RMT Ansatz can be obtained. The different contributions are described by simple diagrams and following an innovative way of partitioning these diagrams we implemented an algorithmic procedure which allows one to easily obtain the Ehrenfest-time dependence. Interestingly this always led to the same factor (which can be traced back to the survival probability only depending on one traversal of each encounter) so that the RMT-type expression is simply modified by the Ehrenfest time by the additional factor ${\rm e}^{-\tau(1-{\rm i}n\epsilon)}$. This is in line with the effective RMT result, but as our result is derived just from the underlying chaotic dynamics of the system we can justify for this situation the use of effective RMT which instead conjectures the Ehrenfest-time dependence.

As the semiclassical framework is based on the underlying classical dynamics we can equally well move away from the RMT arena and obtain the 'classical' contribution to the correlation functions. This can be seen to come from bands of trajectories that remain correlated with each other for the entire duration of their stay inside the system. Furthermore the fact that no mixed (between the RMT-type and classical-type) terms arise is simply due to their opposing classical restrictions. This lack of mixed terms as well as the classical contribution were previously shown to be more generally due to the preservation of volume under the dynamical evolution and the separation of phase-space into two essentially independent subsystems[18,26].

The separation of the correlation functions into two contributions, which each have a straightforward dependence on the Ehrenfest time was previously shown to be responsible for secondary gaps in the density of states of Andreev billiards[27] but equally has an effect on other transport quantities. For the transmission eigenvalues (and their moments) with no energy dependence we just get a straightforward interpolation between the RMT[30] and classical values. For the distribution of the Wigner delay times we further see a truncation of the classical (exponential) distribution and a shift to higher times of the RMT-type distribution. Between the two though a hard gap remains.

The method described in this article allows for the computation of the Ehrenfest-time dependence of the trace of arbitrarily many scattering matrix pairs but only to leading order in inverse channel number $1/N$. The calculation was only doable because at this order the corresponding semiclassical diagrams involve no closed loops and have no periodic orbit encounters (surrounded periodic orbits). When such surrounded periodic orbits

are involved, for example for the conductance variance[34] or the next to leading order quantum correction to the transmission, reflection and the spectral form factor[35], the relatively simple cancellation mechanism observed in this paper no longer holds. But by taking into account all possibilities for partial correlations within the 'fringes' as in Refs. 34,35 in a systematic way, it should however also be possible to extend our Ehrenfest time results to infinite order.

Acknowledgments

The authors thank Cyril Petitjean and Robert Whitney for helpful discussions and acknowledge funding through the Deutsche Forschungsgemeinschaft (Forschergruppe FOR 760) (KR) and the Alexander von Humboldt Foundation (JK).

[1] O. Bohigas, M. J. Giannoni and C. Schmit, Phys. Rev. Lett. **52**, 1 (1984).
[2] M. L. Mehta, *Random matrices, Pure and Applied Mathematics*, Elsevier, Amsterdam (2004).
[3] M. C. Gutzwiller, *Chaos in classical and quantum mechanics*, Springer, New York (1990).
[4] K. Richter, *Semiclassical Theory of Mesoscopic Quantum Systems*, Springer, Berlin (2000).
[5] M. V. Berry, Proc. R. Soc. A **400**, 229 (1985).
[6] J. H. Hannay and A. M. Ozorio de Almeida, J. Phys. A, **17**, 3429 (1984).
[7] M. Sieber and K. Richter, Phys. Scr. T **90**, 128 (2001).
[8] S. Müller, S. Heusler, P. Braun, F. Haake, and A. Altland, Phys. Rev. Lett. **93**, 014103 (2004); Phys. Rev. E **72**, 046207 (2005).
[9] R. Landauer, IBM J. Res. Dev. **1**, 223 (1957); **32**, 306 (1988); M. Büttiker, Phys. Rev. Lett. **57**, 1761 (1986).
[10] R. A. Jalabert, H. U. Baranger, and A. D. Stone, Phys. Rev. Lett. **65**, 2442 (1990); H. U. Baranger, R. A. Jalabert, and A. D. Stone, Phys. Rev. Lett. **70**, 3876 (1993); Chaos **3**, 665 (1993).
[11] K. Richter and M. Sieber, Phys. Rev. Lett. **89**, 206801 (2002).
[12] S. Heusler, S. Müller, P. Braun, and F. Haake, Phys. Rev. Lett. **96**, 066804 (2006); S. Müller, S. Heusler, P. Braun, and F. Haake, New J. Phys. **9**, 1 (2007).
[13] İ. Adagideli, Phys. Rev. B **68**, 233308 (2003).
[14] B. V. Chirikov, F. M. Izrailev, and D. L. Shepelyansky, Sov. Sci. Rev. Sect. C **2**, 209 (1981).
[15] I. L. Aleiner and A. I. Larkin, Phys. Rev. B **54**, 14423 (1996).
[16] P. G. Silvestrov, M. C. Goorden, and C. W. J. Beenakker, Phys. Rev. Lett. **90**, 116801 (2003).
[17] S. Rahav and P. W. Brouwer, Phys. Rev. Lett. **95**, 056806 (2005).
[18] Ph. Jacquod and R. S. Whitney, Phys. Rev. B **73**, 195115 (2006).
[19] O. Agam, I. Aleiner, and A. Larkin, Phys. Rev. Lett. **85**, 3153 (2000).
[20] P. G. Silvestrov, M. C. Goorden, and C. W. J. Beenakker, Phys. Rev. B **67**, 241301(R) (2003).
[21] J. Tworzydło, A. Tajic, H. Schomerus, and C. W. J. Beenakker, Phys. Rev. B **68**, 115313 (2003).
[22] R. S. Whitney and Ph. Jacquod, Phys. Rev. Lett. **96**, 206804 (2006).
[23] M. C. Goorden, P. Jacquod, and C. W. J. Beenakker, Phys. Rev. B **72**, 064526 (2005).
[24] C. W. J. Beenakker, Lect. Notes Phys. **667**, 131 (2005).
[25] P. W. Brouwer and S. Rahav, Phys. Rev. B **74**, 085313 (2006).
[26] R. S. Whitney and Ph. Jacquod, Phys. Rev. Lett. **94**, 116801 (2005).
[27] J. Kuipers, D. Waltner, C. Petitjean, G. Berkolaiko, and K. Richter, Phys. Rev. Lett. **104**, 027001 (2010); J. Kuipers, T. Engl, G. Berkolaiko, C. Petitjean, D. Waltner, and K. Richter, *preprint* arXiv:1004.1327.
[28] Yu. V. Nazarov, *Quantum Noise in Mesoscopic Physics* Kluwer, Dordrecht (2003).
[29] C. Petitjean, D. Waltner, J. Kuipers, İ. Adagideli, and K. Richter, Phys. Rev. B **80**, 115310 (2009).
[30] G. Berkolaiko, J. M. Harrison, and M. Novaes, J. Phys. A **41**, 365102 (2008).
[31] E. P. Wigner, Phys. Rev. **98**, 145 (1955); F. T. Smith, Phys. Rev. **118**, 349 (1960).
[32] G. Berkolaiko and J. Kuipers, J. Phys. A **43**, 035101 (2010).
[33] P. W. Brouwer, K. M. Frahm and C. W. J. Beenakker, Waves in Random Media **9**, 91 (1999).
[34] P. W. Brouwer and S. Rahav, Phys. Rev. B **74**, 075322 (2006).
[35] D. Waltner and J. Kuipers, *preprint* arXiv:1006.0142.